

# Creating and probing the Sachdev-Ye-Kitaev model with ultracold gases: Towards experimental studies of quantum gravity

Ippei Danshita<sup>1,\*</sup>, Masanori Hanada<sup>1,2,3,†</sup> and Masaki Tezuka<sup>4,‡</sup>

<sup>1</sup>*Yukawa Institute for Theoretical Physics, Kyoto University, Kyoto 606-8502, Japan*

<sup>2</sup>*Stanford Institute for Theoretical Physics, Stanford University, Stanford, CA 94305, USA*

<sup>3</sup>*The Hakubi Center for Advanced Research, Kyoto University, Kyoto 606-8501, Japan*

<sup>4</sup>*Department of Physics, Kyoto University, Kyoto 606-8502, Japan*

(Dated: March 15, 2019)

We suggest that the holographic principle, combined with recent technological advances in atomic, molecular, and optical physics, can lead to experimental studies of quantum gravity. As a specific example, we consider the Sachdev-Ye-Kitaev (SYK) model, which consists of spin-polarized fermions with an all-to-all random two-body hopping and has been conjectured to be dual to a certain quantum gravitational system. We propose that the SYK model can be engineered by confining ultracold fermionic atoms into optical lattices and coupling two atoms with molecular states via photo-association lasers. Achieving low-temperature states of the SYK model is interpreted as a realization of a stringy black hole, provided that the holographic duality is true. We also show how to measure out-of-time-order correlation functions of the SYK model, which allow for identifying the maximally chaotic property of the black hole.

## I. INTRODUCTION

The quantum nature of black holes is one of the most important subjects in theoretical physics, since the theoretical discovery of particle-emissions from a black hole due to quantum effects [1, 2], which are often referred to as the Hawking radiation. Although there have been experimental searches for quantum black holes at the CERN LHC motivated by the predictions on the basis of theories of TeV-scale quantum gravity [3–5], no evidence of the black hole creation has been observed thus far [6–9]. In this paper, we present a completely different route to experimental studies of quantum gravity by exploiting both holographic principle and unprecedented controllability of optical-lattice systems loaded with ultracold gases [10].

In order to resolve paradoxes associated with the black hole evaporation that results from the Hawking radiation, the holographic principle [13, 14] emerged, which claims that black holes, and more general quantum gravitational theories, are equivalent to non-gravitational theories in different spacetime dimensions. The gauge/gravity duality conjecture [15] provides us with concrete setups: this conjecture claims that superstring/M-theory on certain spacetimes are equivalent to quantum field theories. Although this conjecture has not been proven yet, it is believed to be correct at least in some simplest cases. For example, maximally supersymmetric matrix quantum mechanics (also known as the Matrix Model of M-theory [16, 17]), which is believed to describe a black hole in type IIA superstring theory near the 't Hooft large- $N$  limit [18], has been studied numerically starting in [19]. The agreement with the dual superstring theory prediction has been confirmed including the effect of virtual loops of string [20]. Note that this is not merely ‘analogy’ nor ‘model’; quantum field theories should be literally equivalent to quantum gravitational systems, which means that they are not distinguishable in principle.

Thanks to their high controllability and cleanness, experiments with ultracold gases in optical lattices have succeeded in realizing various theoretical models, which were introduced in the contexts of condensed matter physics but did not have quantitative experimental counterparts. Examples include the Bose-Hubbard model [22], the Lieb-Liniger model [23, 24], the Aubry-André model [25], the Harper Hamiltonian [26, 27], and the topological Haldane model [28]. There have been theoretical proposals also for realizing lattice gauge models studied in high-energy physics [29, 30]. These circumstances tempt one to expect that it may be possible as well to realize quantum field theories dual to quantum gravitational systems.

In this paper, we propose a possible way to create the Sachdev-Ye-Kitaev (SYK) model [31, 32] experimentally with use of ultracold gases in optical lattices. The SYK model consists of spin-polarized fermions with an all-to-all random two-body hopping. Its thermal state is a non-Fermi liquid with nonzero entropy at vanishing temperature,

---

\*Electronic address: danshita@yukawa.kyoto-u.ac.jp

†Electronic address: hanada@yukawa.kyoto-u.ac.jp

‡Electronic address: tezuka@scphys.kyoto-u.ac.jp

which is called the Sachdev-Ye (SY) state [33], and has been conjectured to be dual to charged black holes with two-dimensional anti-de Sitter ( $\text{AdS}_2$ ) horizons [31, 34]. For the purpose of experimental realization, this model is advantageous over the other known models with holography in the sense that it consists of non-relativistic particles and is not supersymmetric. Here we emphasize that the experimental realization of the SY state in optical-lattice systems is equivalent to that of a quantum black hole if the duality is true. Owing to the flexible controllability and diluteness of the optical-lattice system, it will allow for the first experimental investigation for various important properties of quantum black holes, such as the thermodynamics, the formation and evaporation dynamics, and the chaotic properties.

Our strategy to achieve the SYK model is twofold. We first simplify the model into a form that can be experimentally accessed more easily. Specifically, we numerically demonstrate that the original SYK model, which has a complex two-body hopping with Gaussian randomness, can be quantitatively approximated by the model possessing a real two-body hopping mediated via random couplings to multiple molecular states. Second, we show that the latter model can be created by confining ultracold fermionic atoms into a deep optical lattice and utilizing photo-association (PA) lasers [35] that couple all the combinations of two atomic bands with molecular states. We discuss the feasibility of this proposed scheme by taking  $^6\text{Li}$  and a double-well optical lattice [36, 37] as specific choices of atomic species and lattice configuration. We also present a protocol to measure two physical quantities characterizing the black hole dual to the SY state, namely out-of-time-order correlation (OTOC) functions [32, 38] and single-particle Green's function [31].

The remainder of this paper is organized as follows. In Sec. II, we briefly review the SYK model and modify it in a form more suited for experimental realization with ultracold gases in optical lattices. In Sec. III, we show how to realize the modified SYK model. In Sec. IV, we consider feasible measurements of physical quantities that characterize quantum black holes realized in the proposed scheme. In Sec. V, we summarize the results and discuss future prospects. We set the reduced Planck's constant and the Boltzmann constant to be  $\hbar = k_B = 1$  except in Sec. III.B, where specific values of physical quantities are evaluated.

## II. SACHDEV-YE-KITAIEV MODEL

The SYK model [31, 32] is a model of  $Q$  spin-polarized fermions on  $N$  sites. The Hamiltonian is given by [39]

$$\hat{H} = \frac{1}{(2N)^{3/2}} \sum_{ijkl} J_{ij;kl} \hat{c}_i^\dagger \hat{c}_j^\dagger \hat{c}_k \hat{c}_l, \quad (1)$$

where indices run from 1 to  $N$ , the creation and annihilation operators  $\hat{c}_i^\dagger$  and  $\hat{c}_i$  satisfy the anti-commutation relations

$$\{\hat{c}_i, \hat{c}_j\} = \{\hat{c}_i^\dagger, \hat{c}_j^\dagger\} = 0, \quad \{\hat{c}_i^\dagger, \hat{c}_j\} = \delta_{ij}, \quad (2)$$

and  $J_{ij;kl}$  is a complex Gaussian random coupling constant which satisfies

$$J_{ij;kl} = -J_{ji;kl} = -J_{ij;lk}, \quad (3)$$

$$J_{ij;kl} = J_{kl;ij}^* \quad (4)$$

and

$$\overline{(\text{Re } J_{ij;kl})^2} = \begin{cases} J^2/2 & (\{i, j\} \neq \{k, l\}) \\ J^2 & (\{i, j\} = \{k, l\}) \end{cases}, \quad \overline{(\text{Im } J_{ij;kl})^2} = \begin{cases} J^2/2 & (\{i, j\} \neq \{k, l\}) \\ 0 & (\{i, j\} = \{k, l\}) \end{cases}. \quad (5)$$

Here  $\overline{\phantom{x}}$  stands for the disorder average. This system is strongly coupled when  $J/T$  ( $T$ : temperature) is large. Only planar diagrams survive in  $N \rightarrow \infty$  with  $J$  fixed. In the following we take  $J$  as the unit of energy.

This system, in the large- $N$  and strong coupling limit, has properties strikingly resembling a black hole. Firstly, Sachdev [31] pointed out that this theory has the same entropy density as a black hole in  $\text{AdS}_2$ . He also found the agreement of several correlation functions. Furthermore, Kitaev [32] calculated the Lyapunov exponent and found it has a pattern proposed by Maldacena, Shenker and Stanford [38] for quantum theories with dual gravity description. Namely, the Lyapunov exponent takes the maximum value  $2\pi T$  at strong coupling limit  $J/T \rightarrow \infty$ . Therefore it has been expected that the SYK model is actually equivalent to classical gravity in the large- $N$  limit. Then, because this theory admits the  $1/N$ -expansion, it is natural to expect that  $1/N$  correction describes the effect of loops of strings in a similar way to the case of gauge theories [21, 40].

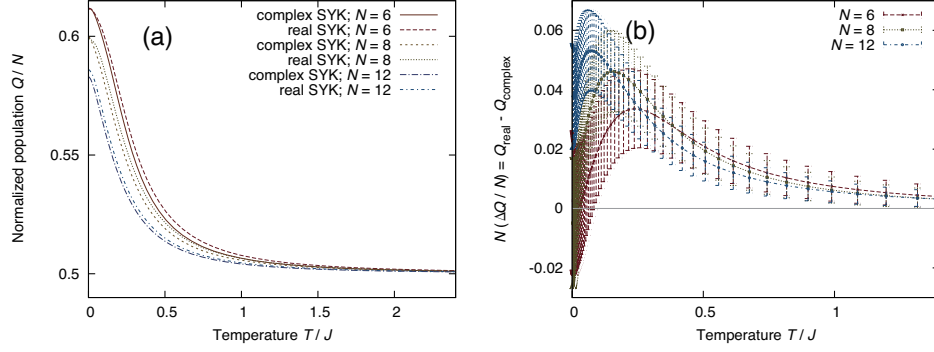


FIG. 1: (a) Comparison of the  $(T/J)$ -dependence of  $\overline{Q}/N$  between the real SYK and the original (complex) SYK models for different  $N$ . (b) The difference of  $\overline{Q}$  between the real and complex SYK models, which is  $N$  times the difference between the values of  $\overline{Q}/N$ . The chemical potential is set to zero, i.e.,  $\mu = 0$ .  $10^3$  samples are taken for  $N = 6, 8$ , and  $12$ .

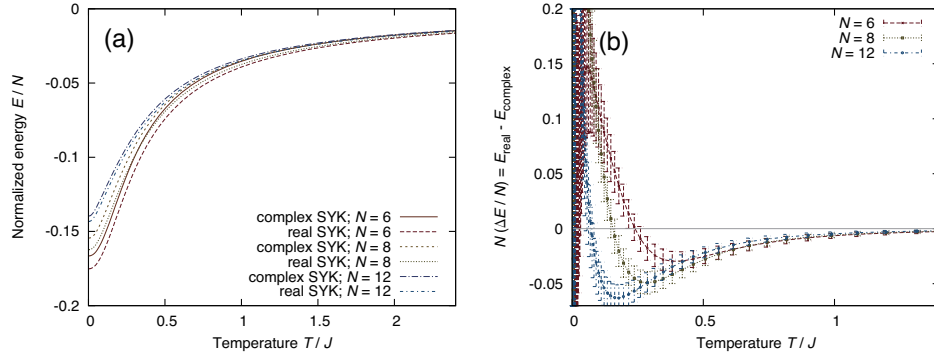


FIG. 2: (a) Comparison and (b) difference of  $(T/J)$ -dependence of  $\overline{E}$  between complex and real SYK models and different  $N$ . The chemical potential is set to zero, i.e.,  $\mu = 0$ .  $10^3$  samples are taken for  $N = 6, 8, 12$ .

### A. From complex $J_{ij,kl}$ to real $J_{ij,kl}$

We slightly modify the SYK model in order to make the experimental implementation easier. The Hamiltonian is still (1), but the random coupling  $J_{ij,kl}$  is taken to be real. Note also that this new theory has time-reversal symmetry, which is important for measurement of the chaotic behaviors.

The Gaussian random coupling is modified to

$$J_{ij;kl} = -J_{ji;kl} = -J_{ij;lk}, \quad (6)$$

$$J_{ij;kl} = J_{kl,ij} \quad (7)$$

$$\overline{|J_{ij;kl}|^2} = \begin{cases} J^2 & (\{i, j\} \neq \{k, l\}) \\ 2J^2 & (\{i, j\} = \{k, l\}) \end{cases}, \quad (8)$$

and for  $\{i, j\} \neq \{k, l\}$

$$\overline{J_{ij,kl} J_{pq,rs}} = J^2 \{(\delta_{ir} \delta_{js} - \delta_{is} \delta_{jr}) (\delta_{kp} \delta_{lq} - \delta_{kq} \delta_{lp}) + (\delta_{ip} \delta_{jq} - \delta_{iq} \delta_{jp}) (\delta_{kr} \delta_{ls} - \delta_{ks} \delta_{lr})\}. \quad (9)$$

Coefficients have been chosen so that the eigenenergy distribution coincides with that of the original SYK model. The second term inside  $\{\dots\}$  in (9) is absent in the original SYK model. Due to this, each Feynman diagram receives some correction after disorder average. However such corrections are  $1/N$ -suppressed in general, and hence this modified model agrees with the original model at large- $N$ . In the following, we call the original SYK model with complex  $J_{ij,kl}$  and the modified one with real  $J_{ij,kl}$  ‘complex-SYK’ and ‘real-SYK,’ respectively.

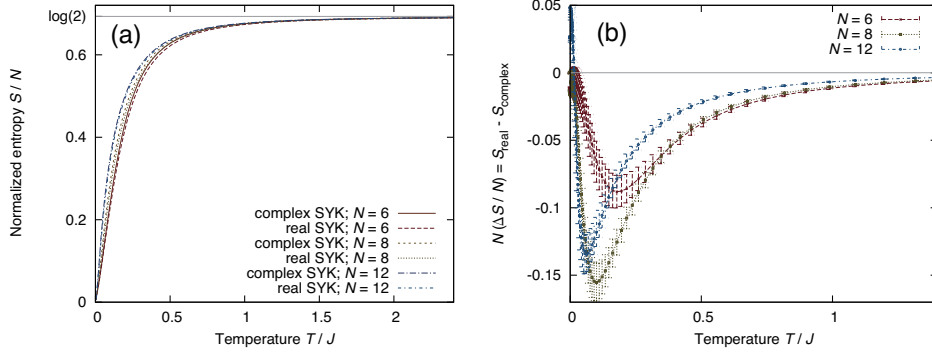


FIG. 3: (a) Comparison and (b) difference of  $(T/J)$ -dependence of  $\overline{S}/N$  between complex and real SYK models and different  $N$ . The chemical potential is set to zero,  $\mu = 0$ . The entropy approaches  $S = N \log 2$  as the temperature  $T$  is increased, which is expected from the fact that all  $2^N$  states can equally contribute in the high-temperature limit.

In Fig. 1, the  $(T/J)$ -dependence of  $Q/N$  in the complex and real SYK model is shown, where  $Q$  denotes the number of fermions, or the charge, defined as the eigenvalue of the number operator  $\hat{Q} = \sum_{i=1}^N \hat{n}_i = \sum_{i=1}^N \hat{c}_i^\dagger \hat{c}_i$  that commutes with all the Hamiltonians considered here. We label the energy eigenvalues of each model Hamiltonian by the charge as  $\{E_i^{(Q)}\}_i$  and obtain

$$\langle Q \rangle_{T,J} = \frac{\sum_Q Q \cdot Z^{(Q)}}{\mathcal{Z}}, \quad (10)$$

in which  $Z^{(Q)}$  is the canonical partition function  $Z^{(Q)} = \sum_i e^{-E_i^{(Q)}/T}$  and  $\mathcal{Z} = \sum_Q Z^{(Q)}$  is the grandcanonical partition function. In Fig. 2, the  $(T/J)$ -dependence of the energy in the complex and real-SYK models, normalized by dividing by  $N$ , are shown. The energy  $E$  is calculated as

$$\langle E \rangle_{T,J} = \frac{\sum_{Q,i} E_i^{(Q)} \cdot e^{-E_i^{(Q)}/T}}{\mathcal{Z}}. \quad (11)$$

The disorder average  $\overline{\langle E \rangle}$  and  $\overline{\langle Q \rangle}$  are taken by using random couplings. From the plots, we can see a clear agreement at large- $N$ . As expected from the standard  $1/N$ -counting, two theories give the same values of  $\overline{\langle E \rangle}$  and  $\overline{\langle Q \rangle}$  up to the sub-leading corrections of order  $N^0$ .

We have also calculated the entropy  $S$  defined by

$$\overline{S} = \frac{\overline{\langle E \rangle}}{T} + \log \overline{\mathcal{Z}}. \quad (12)$$

Note that  $\log \overline{\mathcal{Z}} < \log \mathcal{Z}$  in general. The result is shown in Fig. 3. For  $T/J \gtrsim 1$ ,  $S/N$  is already almost converged at  $N = 6$ , while for smaller  $T$ ,  $S/N$  is an increasing function of  $N$ . Notice that the entropy of the complex SYK model at finite  $N$  has been computed also in Ref. [41].

As an example of a two-point function, in Fig. 4 we present the same-site density-density correlation function  $C_{\text{nn}}(t)$ , which is defined using the number operator  $\hat{n}_i = \hat{c}_i^\dagger \hat{c}_i$  by

$$C_{\text{nn}}^{(i)}(t) = \overline{\langle \hat{n}_i(t) \hat{n}_i(0) \rangle} - \overline{\langle \hat{n}_i(t) \rangle} \cdot \overline{\langle \hat{n}_i(0) \rangle} = \overline{\langle \hat{n}_i(t) \hat{n}_i(0) \rangle} - \overline{\langle \hat{n} \rangle}^2 \equiv \overline{\langle \hat{n}_i(t) \hat{n}_i(0) \rangle}_{\text{conn}}; \quad (13)$$

$$C_{\text{nn}}(t) = \frac{1}{N} \sum_i C_{\text{nn}}^{(i)}(t). \quad (14)$$

Here, the operator  $\hat{\mathcal{O}}(t)$  at time  $t$  is  $\hat{\mathcal{O}}(t) = e^{i\hat{H}t} \hat{\mathcal{O}} e^{-i\hat{H}t}$  and the expectation values are calculated as in the cases of the charge and the energy:

$$\langle \dots \rangle = \frac{\sum_{Q,j} e^{-\beta E_j^{(Q)}} \langle \psi_j^{(Q)} | \dots | \psi_j^{(Q)} \rangle}{\mathcal{Z}} \quad (15)$$

with  $|\psi_j^{(Q)}\rangle$  being the many-body wavefunction corresponding to the eigenenergy  $E_j^{(Q)}$ .

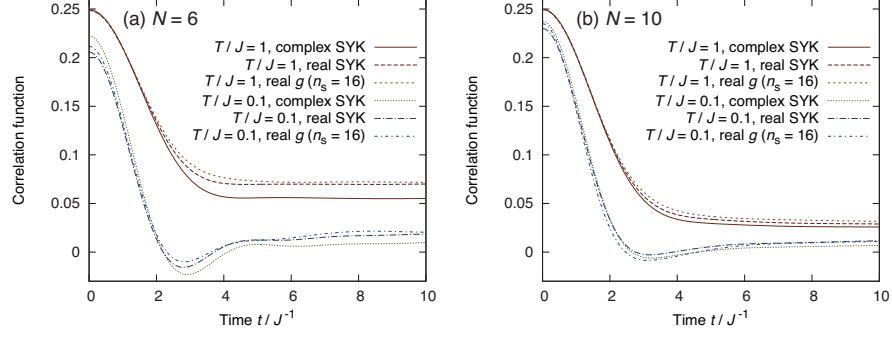


FIG. 4: The real-time, same-site density-density correlation function  $\sum_i \langle \hat{n}_i(t) \hat{n}_i(0) \rangle - \langle \hat{n}_i(t) \rangle \langle \hat{n}_i(0) \rangle / N$  calculated for (a)  $N = 6$  using  $10^3$  samples, and (b)  $N = 10$  using  $10^2$  samples. The data for  $T = 1$  and  $0.1$  for the complex SYK and the real SYK models are plotted together with the data for the model (17).

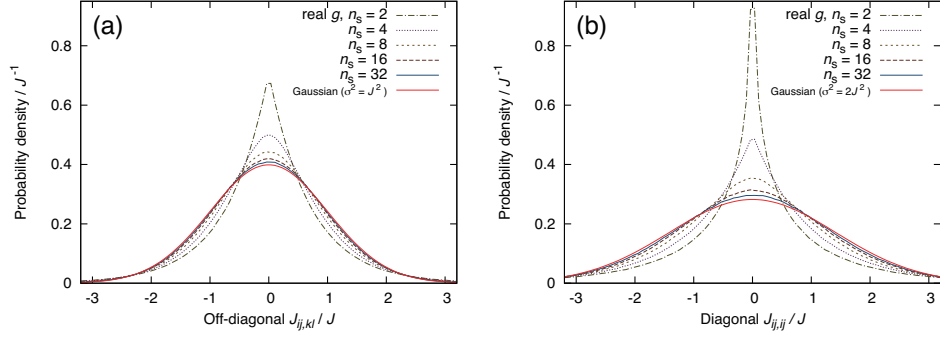


FIG. 5: (a): Distribution of  $J_{ij,kl} = \frac{(2N)^{3/2}}{\sqrt{n_s}J} (\sum_{s:\text{even}} g_{s,ij} g_{s,kl} - \sum_{s:\text{odd}} g_{s,ij} g_{s,kl})$  with only the off-diagonal components (i.e.  $(i,j) \neq (k,l), (l,k)$ ); (b): Distribution of  $J_{ij,ij} = \frac{(2N)^{3/2}}{\sqrt{n_s}J} (\sum_{s:\text{even}} g_{s,ij}^2 - \sum_{s:\text{odd}} g_{s,ij}^2)$ . The weight of real  $g_{s,ij}$  is Gaussian,  $\frac{e^{-g_{s,ij}^2/(2\sigma_g^2)}}{\sqrt{2\pi}\sigma_g}$  with  $\sigma_g^2 = (2N)^{-3/2} J^2$ . The distribution of  $J_{ij,kl}$  converges to  $\frac{e^{-(\text{Re } J_{ij,kl})^2/(2J^2)}}{\sqrt{2\pi}J}$ , which is shown in (a) as “Gaussian ( $\sigma^2 = J^2$ )”. The distribution of  $J_{ij,ij}$  converges to  $\frac{e^{-J_{ij,ij}^2/(4J^2)}}{\sqrt{4\pi}J}$ , as shown in (b) as “Gaussian ( $\sigma^2 = 2J^2$ )”.  $N = 10$ . The numbers of samples taken are  $10^4$  (a) and  $10^5$  (b), respectively.

### B. $J_{ij,kl}$ term mediated by multiple molecular states

One of the most severe bottlenecks for realizing the SYK model in optical-lattice experiments is the implementation of the all-to-all two-body hopping, because particles on lattice systems in general move the most dominantly via nearest-neighboring one-body hopping. In order to overcome this bottleneck, we consider a situation, in which two atoms are coupled with  $n_s$  molecular states, described by the following Hamiltonian,

$$\hat{H}_m = \sum_{s=1}^{n_s} \left\{ \nu_s \hat{m}_s^\dagger \hat{m}_s + \sum_{i,j} g_{s,ij} \left( \hat{m}_s^\dagger \hat{c}_i \hat{c}_j - \hat{m}_s \hat{c}_i^\dagger \hat{c}_j^\dagger \right) \right\}. \quad (16)$$

By integrating  $\hat{m}_s$  out, we obtain the following effective Hamiltonian,

$$\hat{H}_{\text{eff}} = \sum_{s,i,j,k,l} \frac{g_{s,ij} g_{s,kl}}{\nu_s} \hat{c}_i^\dagger \hat{c}_j^\dagger \hat{c}_k \hat{c}_l. \quad (17)$$

A similar way of designing a kind of two-body hopping term, namely the ring exchange interaction, by means of intermediate two-particle states has been pointed out in previous work [42]. In the next section we elaborate how to prepare such a situation in optical-lattice systems while in this section we show that Eq. (17) serves as a quantitative approximation of the complex SYK model (1) when  $n_s$  is sufficiently large and  $\nu_s$  is appropriately tuned. It is worth stressing the importance of large  $n_s$ . Even when  $n_s = 1$ , the model (17) looks like the real-SYK model if we identify  $J_{ij,kl}/(2N)^{3/2}$  with  $g_{ij} g_{kl}/\nu$ , where  $g_{ij} \equiv g_{1,ij}$  and  $\nu \equiv \nu_1$ . However, the distribution of the latter is not Gaussian in

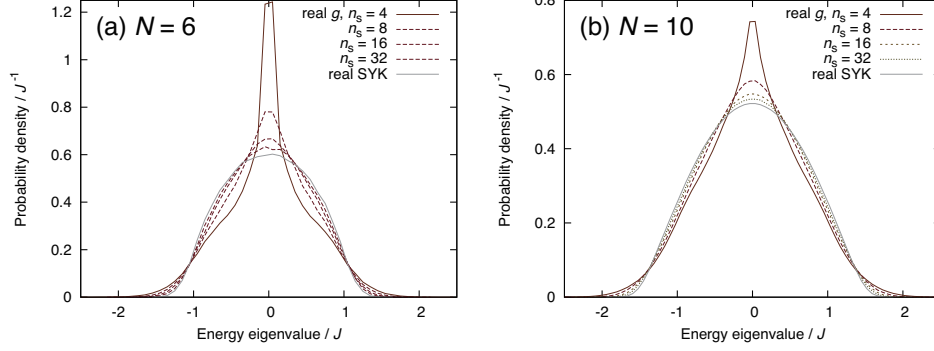


FIG. 6: The energy spectrum with real  $g_{ij}$ ,  $\nu_s = +\sqrt{n_s}J$  for even  $s$  and  $\nu_s = -\sqrt{n_s}J$  for odd  $s$  for (a)  $N = 6$  and (b)  $N = 10$ , particle number  $Q = N/2$ , and for different values of  $n_s$ . The weight of  $g_{s,ij}$  is chosen to be  $\frac{e^{-g_{s,ij}^2/(2\sigma_g^2)}}{\sqrt{2\pi}\sigma_g}$ .  $10^4$  samples for each.

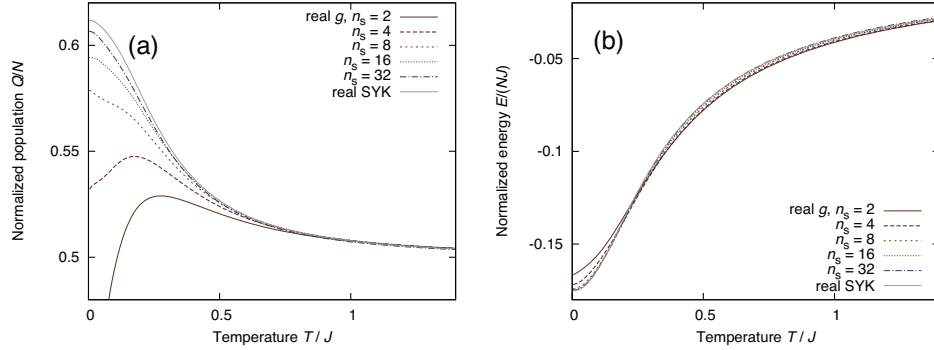


FIG. 7: The  $(T/J)$ -dependence of (a)  $\overline{Q}$  and (b)  $\overline{E}$  for  $N = 6$  for  $n_s = 2, 4, 8, 16, 32$ . The chemical potential is set to zero,  $\mu = 0$ . The results for the real SYK model are shown for comparison.  $10^4$  samples are used and the standard error estimates (not shown) are typically on the order of the width of the lines.

general for a given distribution of  $\{g_{ij}\}$  and even worse, i.e., the randomness is not strong enough; for example, when  $g_{12}g_{12}/\nu$  and  $g_{34}g_{34}/\nu$  are large,  $g_{12}g_{34}/\nu$  is also large. Note also that  $g_{ij}g_{ij}$  is always positive.

Let us suppose  $\nu_1 = \nu_2 = \dots = \nu_{n_s} \propto \sqrt{n_s}$ . Then, if  $n_s$  is large enough,  $\sum_s \frac{g_{s,ij}g_{s,kl}}{\nu_s}$  should become Gaussian except for the diagonal elements  $(i, j) = (k, l)$  or  $(i, j) = (l, k)$  (note that  $g_{s,ij}^2$  is always positive). This happens because it is simply an  $n_s$ -step random walk for each set of indices  $(i, j, k, l)$ . In order to improve the behavior of the diagonal elements, we take  $n_s$  to be even, and set  $\nu_s = +\sqrt{n_s}\sigma_s$  for even  $s$  and  $\nu_s = -\sqrt{n_s}\sigma_s$  for odd  $s$ . We assume that the distribution of the real  $g_{s,ij}$  is Gaussian having the variance  $\sigma^2 = \sigma_g^2$ , with  $\sigma_g^2/\sigma_s = J/(2N)^{3/2}$ . In the following we set  $\sigma_s = \sigma_g = J/(2N)^{3/2}$  for simplicity.

As explained in Appendix A, if we identify  $\sum_s \frac{g_{s,ij}g_{s,kl}}{\nu_s}$  defined in this way with  $J_{ij,kl}/(2N)^{3/2}$ , the properties needed in the real-SYK model are satisfied at  $n_s = \infty$ . For  $N = 10$ , we collected samples by using independent real Gaussian random values of  $\{g_{ij}\}$ . In Fig. 5, we plot the distribution of  $J_{ij,kl}$  with  $\{i, j\} \neq \{k, l\}$  and  $10^4$  samples (a) and the diagonal elements  $J_{ij,ij}$  with  $10^5$  samples (b). The distributions have different shapes for smaller values of  $n_s$ , but they quickly approach Gaussian distributions with corresponding variances for the original SYK model as  $n_s$  is increased.

In Fig. 6 we plot the energy spectrum of this model using  $10^4$  samples, with (a)  $N = 6$  and (b)  $N = 10$ , and the number of fermions fixed to  $Q = N/2$ . The energy spectra become closer to each other and to that of the SYK model as the number of molecular state  $n_s$  increases. As shown in Fig. 7 for  $\overline{Q}$  and  $\overline{E}$ , we observe that the results are already similar for  $n_s = 8$  for  $N = 6$  and 10. In Fig. 8 (a) we plot the entropy  $\overline{S}$  as a function of the temperature for  $N = 6, 8, 12$  for  $n_s = 16$ , along with the result of linear extrapolation to  $1/N \rightarrow 0$ . As in Fig. 8 (b), for  $T \gtrsim 0.1J$  the obtained entropy is almost linear in  $1/N$ , however for lower temperatures the dependence of  $\overline{S}$  on  $1/N$  is more convex, indicating that the linear fit from  $N = 6, 8, 12$  may be underestimating the value of  $\overline{S}(N \rightarrow \infty)$  at  $T \rightarrow 0$  and that  $\overline{S}$  may converge to a finite value.

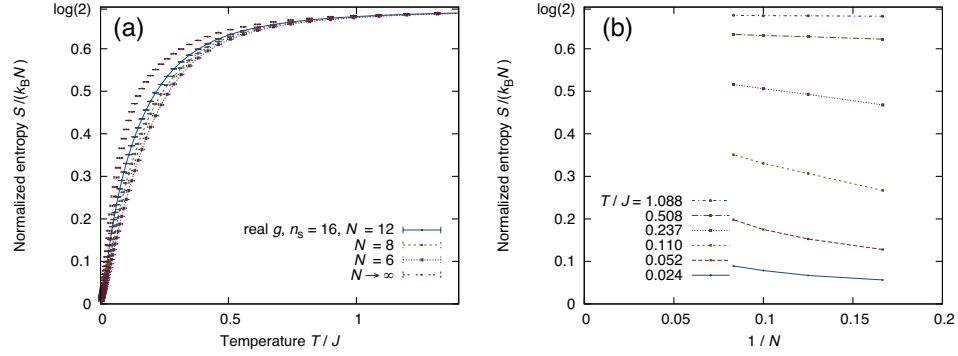


FIG. 8: (a) Comparison of the  $(T/J)$ -dependence of  $\overline{S}/(k_B N)$ , the complex-SYK model and the real modified SYK model with  $n_s = 16$ , extrapolated to  $N = \infty$  by a linear fit of the value against  $1/N$ . The chemical potential is set to zero,  $\mu = 0$ . (b)  $\overline{S}/(k_B N)$  plotted against  $1/N$  for  $N = 6, 8, 12$ . For higher  $T$  the obtained normalized entropy is linear in  $1/N$ , however for  $T/J \ll 1$  the curve is more convex, which suggests that the actual  $N \rightarrow \infty$  limit may be significantly larger than the value plotted and may converge to a finite value as  $T \rightarrow 0$ .

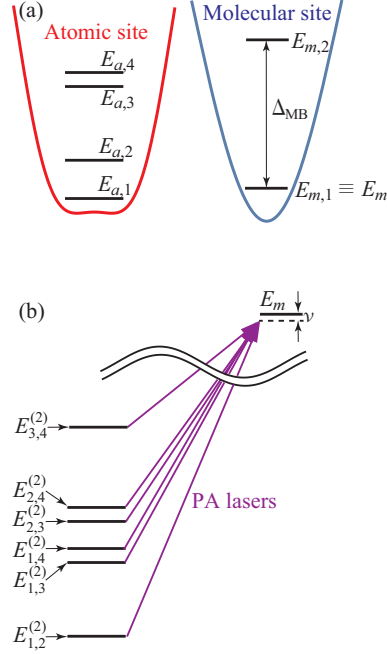


FIG. 9: Schematic illustrations of the energy levels of the atomic and molecular states relevant to our protocol (a) and the PA process (b) for  $N = 4$ .

### III. CREATING THE MODEL

#### A. General scheme

In this section, we explain how to create the model (17), a simplified version of the SYK model, in a system of optical lattices loaded with ultracold gases. We consider a two-dimensional gas of spin-polarized fermionic atoms confined in an optical lattice. In the proposed scheme, we utilize the PA process that coherently converts two atoms into a bosonic molecule in a certain electronic (or hyperfine), vibrational, and rotational state [35]. Since in general the lattice depth for molecules may be controlled independently from that for atoms, we assume that the former has the sign opposite to the latter. In this situation, the potential minima of the molecular optical lattice sit right next to those of the atomic optical lattice, as illustrated in Fig. 9(a), such that we do not have to take into account the effects of the onsite interactions between an atom and a molecule, which would otherwise complicate the levels of the atomic and molecular bands. We assume that the optical lattices are so deep that atoms and molecules in each lattice site



are completely isolated. To make the manipulation of the system easier, we remove all the atoms in the lattice sites neighboring to occupied sites. We also assume that each occupied atomic lattice site contains  $Q$  atoms. We regard the band degrees of freedom in the atomic site as the physical site index of the SYK model. More specifically, the first, second, third,  $\dots$ ,  $N$ -th bands correspond to  $i = 1, 2, 3, \dots, N$  sites. We write the energy of the lowest molecular band and that of the  $i$ -th atomic band as  $E_m$  and  $E_{a,i}$ .

Let us introduce a PA laser, which couples atomic bands  $i(\leq N)$  and  $j(\leq N)$  with the lowest molecular band. The frequency of the PA laser is chosen as

$$\omega_{i,j}^{\text{PA}} = E_m - E_{i,j}^{(2)} - \nu, \quad (18)$$

where  $E_{i,j}^{(2)} = E_{a,i} + E_{a,j}$ , and  $\nu$  denotes the detuning. We consider a situation in which all the combinations of the two atomic bands  $(i, j)$  are coupled via independent PA lasers as shown in Fig. 9(b). For such a situation to be possible,  $|\nu|$  has to be larger than the linewidth of the PA lasers  $\Gamma_{\text{PA}}$  and that of the molecular state  $\Gamma_{\text{ms}}$ . In addition, the condition  $|\nu| \ll \Delta_{\min}$  has to be satisfied, where  $\Delta_{\min}$  denotes the minimum level spacing in  $E_{i,j}^{(2)} \leq E_{N-1,N}^{(2)}$ . The number of necessary PA lasers is  $N(N-1)/2$ . The PA process is described by the following Hamiltonian,

$$\hat{H}_{\text{m1}} = \nu \hat{m}^\dagger \hat{m} + \sum_{i,j} g_{ij} (\hat{m}^\dagger \hat{c}_j \hat{c}_i + h.c.), \quad (19)$$

where the atom-molecule coupling constant is given by

$$g_{ij} = \frac{1}{2} \text{sgn}(j-i) \int d\mathbf{r} \Omega_{i,j}(\mathbf{r}) w_m(\mathbf{r}) w_{a,i}(\mathbf{r}) w_{a,j}(\mathbf{r}). \quad (20)$$

$\Omega_{i,j}(\mathbf{r})$  denotes the intensity of the PA laser while  $w_m(\mathbf{r})$  and  $w_{a,i}(\mathbf{r})$  represent the Wannier function of the 1st molecular band and the  $i$ -th atomic band. The absolute value of the detuning  $|\nu|$  is assumed to be much smaller than the onsite interaction  $U$  between two molecules in order to avoid double occupancy of the molecules. For the same reason,  $U$  has to be much smaller than the minimum level spacing  $\Delta_{\min}$  in  $E_{i,j}^{(2)}$  or sufficiently larger than the maximum level spacing  $\Delta_{\max}$  in  $E_{i,j}^{(2)}$ . Moreover, the level spacing between the first and second molecular bands  $\Delta_{\text{MB}}$  is assumed to be larger than  $\Delta_{\max}$  in order to avoid accidental couplings between higher molecular bands and the atomic bands via the PA lasers.

A PA molecule has many vibrational and rotational states. When  $\Delta_{\max} < \tilde{\Delta}$ , we can extend the scheme described above to include couplings of two atoms with multiple molecular states, where  $\tilde{\Delta}$  denotes the minimum level spacing of the involved molecular states. The extended system is now described by Eq. (16). When  $|\nu_s| \gg \max(g_{s;ij})$ , one can integrate out the molecular degrees of freedom through the second-order perturbation theory with respect to the atom-molecule couplings, leading to the effective Hamiltonian of Eq. (17). We emphasize that the coupling constant  $g_{s;ij}$  can be controlled independently with respect to indices  $s$ ,  $i$ , and  $j$  because each coupling is created via an independent PA laser. Setting  $\nu_s$  to be bimodal,  $\sqrt{n_s}\sigma_s$  for even  $s$  and  $-\sqrt{n_s}\sigma_s$  for odd  $s$ , and the distribution function of  $g_{s;ij}$  to be Gaussian as

$$f(g_{s;ij}) = \frac{1}{\sqrt{2\pi}\sigma_g} e^{-\frac{(g_{s;ij})^2}{2\sigma_g^2}}, \quad (21)$$

the coupling  $J_{ij;kl} \equiv (2N)^{3/2} \sum_s g_{s;ij} g_{s;kl} / \nu_s$  becomes Gaussian random for sufficiently large  $n_s$  as shown in the previous section, where  $\sigma_g^2 / \sigma_s = J / (2N)^{3/2}$ . Thus, we claim that the simplified SYK model of Eq. (17) may be created with this scheme. In the following we set  $\sigma_s = \sigma_g = J / (2N)^{3/2}$  for simplicity.

It is useful to summarize the necessary conditions for this scheme to be valid in terms of the several relevant energy scales,

$$\max(t_i) \lesssim \hbar / \tau_{\text{exp}} \ll J, \quad (22)$$

$$\max(\hbar \Gamma_{\text{PA}}, \hbar \Gamma_{\text{ms},s}) \ll |\nu_s| \ll \Delta_{\min}, \text{ for all } s, \quad (23)$$

$$\Delta_{\max} < \Delta_{\text{MB}} < \tilde{\Delta}, \quad (24)$$

$$|\nu_s| \ll |U_{s,s'}|, \text{ for all } s \text{ and } s', \quad (25)$$

$$|U_{s,s'}| < \Delta_{\min} \text{ or } \Delta_{\max} < |U_{s,s'}|, \text{ for all } s \text{ and } s'. \quad (26)$$

Here  $U_{s,s'}$ ,  $t_i$ , and  $\tau_{\text{exp}}$  denote the onsite interaction between two molecules in states  $s$  and  $s'$ , the intersite hopping for atoms in the  $i$ -th band, and the lifetime of the experimental system, which is approximately a few seconds in typical experiments of ultracold gases in optical lattices. Notice that the total number of necessary PA lasers in this scheme is  $n_s \times N(N-1)/2$ .



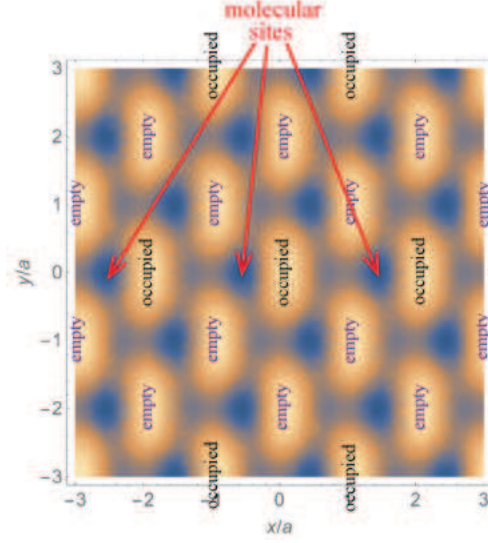


FIG. 10: Spatial profile of the optical lattice of Eq. (27) for  $V_0 < 0$ ,  $R = 0.59$ , and  $\theta = \pi/6$ . The dark and light colors indicate the high- and low-potential regions. This means that the lightest (darkest) spots correspond to the atomic (molecular) sites.

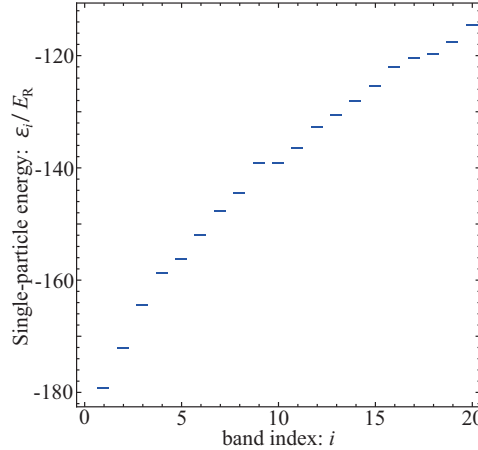


FIG. 11: Eigenenergies of the Schrödinger equation for a single atom in the optical-lattice potential of Eq. (27) at zero quasi-momentum, where  $V_0 = -60 E_R$ ,  $R = 0.59$ , and  $\theta = \pi/6$ . From this energy spectrum, one can evaluate that  $\Delta_{\min} = 0.00228 E_R$  and  $\Delta_{\max} = 104 E_R$  for  $N = 16$ .

### B. An example: double-well optical lattice

As a specific example, we consider the following optical lattice,

$$V_{\text{ol}}(\mathbf{r}) = V_0 \left[ \cos^2 \left( \frac{\pi x}{a} \right) + \sin^2 \left( \frac{\pi y}{a} \right) + R \left( \cos \left( \frac{\pi x}{a} - \theta \right) + \cos \left( \frac{\pi y}{a} \right) \right)^2 \right]. \quad (27)$$

This optical lattice consists of two square optical lattices and  $a$  represents the lattice spacing of the one with the shorter period. We assume that  $V_0 < 0$  for atoms while  $V_0 > 0$  for molecules. In Fig. 10 we show the spatial profile of this potential for  $V_0 < 0$ ,  $R = 0.59$ , and  $\theta = \pi/6$ . Such an optical lattice is often used to create a double-well optical lattice [36, 37], whose unit cell is a double well potential, and is advantageous for the proposed scheme in the sense that the band levels of the atomic site have no degeneracy as shown in Fig. 11, where the eigenenergies of a single atom in the optical lattice at zero quasi-momentum are plotted for  $V_0 = -60 E_R$ ,  $R = 0.59$ , and  $\theta = \pi/6$ .  $E_R \equiv \frac{\hbar^2 \pi^2}{2ma^2}$  denotes the recoil energy. If there are any degenerate levels, then  $\Delta_{\min} = 0$  such that the condition (23) can not be satisfied.

To evaluate the energy scales appearing in the necessary conditions (22)-(26), let us specifically choose  $^6\text{Li}$  as the

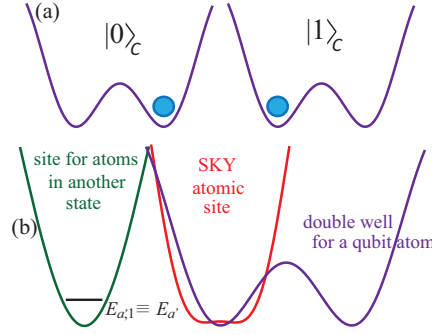


FIG. 12: Schematic illustrations of the qubit states (a) and the configuration for measuring the OTOC functions of Eq. (29) (b).

fermionic atoms confined in our system. Use of this species in cold-atom experiments is rather standard. Setting the lattice spacing to be a standard value, namely  $d = 532\text{nm}$ , leads to the recoil energy  $E_R = h \times 29.2\text{kHz}$ . Taking the values of the parameters used in Fig. 11 and setting  $N = 16$  immediately give  $\max(t_i) \sim h \times 0.5\text{Hz}$ ,  $\Delta_{\min} = h \times 2.02\text{kHz}$ , and  $\Delta_{\max} = h \times 1.96\text{MHz}$ . If we set  $|\nu_\eta| = h \times 10\text{Hz}$  and  $n_{\text{ms}} = 36$ , then  $J = h \times 300\text{Hz}$ . Hence, the first condition (22) is safely satisfied.

Since the second condition (23) requires the information of the linewidths, let us first estimate  $\Gamma_{\text{ms}}$ . If a PA molecule consists of one electronically ground-state alkali atom and one electronically excited alkali atom, a typical scale of the linewidth is  $\Gamma_{\text{ms}} \sim 2\pi \times 10\text{MHz}$  [35], which is much larger than  $|\nu_\eta|$  and can not be used for the present scheme. In contrast, if a PA molecule consists of two electronically ground-state alkali atoms,  $\Gamma_{\text{ms}} \sim 2\pi \times 0.1\text{Hz}$  [43]. As for  $\Gamma_{\text{PA}}$ , state-of-art experiments have developed lasers with ultra-narrow linewidth for application to optical-lattice atom clocks such that the linewidth can be as low as  $\Gamma_{\text{PA}} \sim 2\pi \times 0.1\text{Hz}$  [44–46]. Using the electronically ground-state molecules and the state-of-art lasers, the condition (23) can be overcome.

Furthermore, we assume that  $V_0 = 2 \times 10^5 E_R$  for the molecular optical lattice so that  $\Delta_{\text{MB}} = h \times 10.9\text{MHz}$ . Since the level spacing of the rotational states of a  ${}^6\text{Li}_2$  molecule is typically  $\tilde{\Delta} \sim h \times 100\text{MHz}$ , the third condition (24) is also satisfied. Finally, we estimate that  $|U_{s,s'}| \sim 3\text{MHz}$  under the assumption that the s-wave scattering lengths between two molecules take a typical value  $|a_s| \sim 100a_B$ , where  $a_B$  denotes the Bohr radius. With this estimation of  $|U_{s,s'}|$ , the fourth and fifth conditions (25) and (26) are satisfied. This means that it is possible to create the modified SYK model of Eq. (17) at least up to  $N = 16$  by means of the proposed scheme with the specific choices of the optical lattice potential of Eq. (27) and the atomic species of  ${}^6\text{Li}$ .

#### IV. MEASURING OBSERVABLES

Once the SYK model is realized in optical-lattice systems, various observables can be measured. One of the most interesting signatures of a black hole formation is the fast scrambling quantified by OTOC functions [38], with which the chaotic nature of the system can be studied quantitatively. Recently, Swingle *et al.* have proposed a general protocol to measure the OTOC functions [47],

$$F(t) = \langle \hat{W}^\dagger(t) \hat{V}^\dagger(0) \hat{W}(t) \hat{V} \rangle. \quad (28)$$

We follow the protocol to explain how to measure the OTOC functions in our system in the specific case that  $\hat{V} = \hat{c}_i$  and  $\hat{W} = \hat{c}_j$ , namely

$$C_{i,j}(t) = \langle \hat{c}_j^\dagger(t) \hat{c}_i^\dagger(0) \hat{c}_j(t) \hat{c}_i(0) \rangle. \quad (29)$$

Since the SYK model is homogeneously random and has no meaningful distance, this correlation function takes only two different cases, namely the onsite case ( $i = j$ ) and the offsite case ( $i \neq j$ ). Hence, it is sufficient to show the cases that  $i, j \in \{1, N\}$ .

The protocol requires a control qubit interacting with the probed system [47]. We assume that a double-well occupied by a single atom plays the role of a control qubit and regard the state in which the atom occupies the right (left) well as the  $|0\rangle_c$  ( $|1\rangle_c$ ) state of the qubit as shown in Fig. 12(a). We also assume that the species of the qubit atoms is different from that of the SYK atoms and that the optical lattice potential for the former can be controlled independently from that for the latter. We locate the qubit double well in such a way that its left well

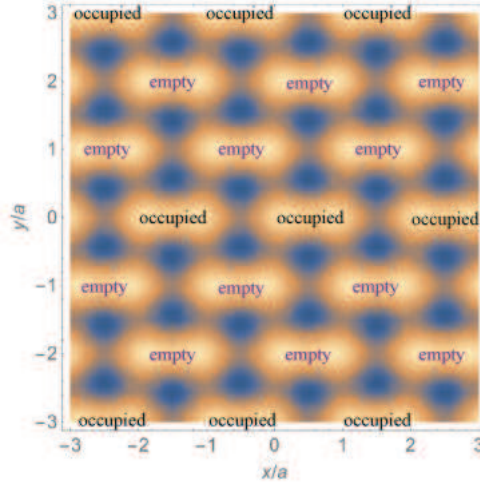


FIG. 13: Spatial profile of the optical lattice of Eq. (30) for qubit atoms, where  $V'_0 < 0$  and  $R = 0.3$ . The dark and light colors indicate the high- and low-potential regions. This means that the lightest spots correspond to the sites for the qubit atoms.

is well overlapped with the site for the SYK atoms [see Fig. 12(b)]. In this situation, the qubit atom has the onsite interactions  $\tilde{U}_i$  with the SYK atom in band  $i$  when the qubit state is  $|1\rangle_C$ . Specifically, supposing that the optical lattice for the SYK atoms is given by Eq. (27), that for the qubit atoms may be formed by the following double-well optical lattice [36, 37],

$$V_{\text{qb}}(\mathbf{r}) = V'_0 \left[ \cos^2 \left( \frac{\pi x}{a} \right) + \cos^2 \left( \frac{\pi y}{a} \right) + R' \left( \sin \left( \frac{\pi x}{a} \right) + \cos \left( \frac{\pi y}{a} \right) \right)^2 \right], \quad (30)$$

whose spatial distribution for  $V'_0 < 0$  and  $R' = 0.3$  is depicted in Fig. 13.

The protocol to measure  $C_{i,j}(t)$  is summarized as follows:

- (i) Prepare  $(|0\rangle_C + |1\rangle_C)/\sqrt{2}$ ,
- (ii)  $\hat{I}_S \otimes |0\rangle\langle 0|_C + \hat{c}_i \otimes |1\rangle\langle 1|_C$ ,
- (iii)  $e^{-i\hat{H}t} \otimes \hat{I}_C$ ,
- (iv)  $\hat{c}_j \otimes \hat{I}_C$ ,
- (v)  $e^{i\hat{H}t} \otimes \hat{I}_C$ ,
- (vi)  $\hat{c}_i \otimes |0\rangle\langle 0|_C + \hat{I}_S \otimes |1\rangle\langle 1|_C$ ,
- (vii) Measure  $\hat{X}_C$  or  $\hat{Y}_C$ ,

where  $\hat{I}$  denotes the identity matrix.  $\hat{X}_C$  and  $\hat{Y}_C$  denote the  $x$  and  $y$  components of the Pauli matrices for the control qubit. Taking the offsite case that  $i = 1$  and  $j = N$ , let us elaborate this protocol item by item. The onsite case can be treated in a very similar way. First, since  $(|0\rangle_C + |1\rangle_C)/\sqrt{2}$  is the ground state of an atom in the symmetric double well for  $\tilde{U}_i = 0$ , it can be straightforwardly prepared by turning off  $\tilde{U}_i$  with use of the Feshbach resonance.

In process (ii), we need to annihilate an atom at site  $i$  when the qubit state is  $|1\rangle_C$ . For this purpose, we prepare a lattice site for an atom in another state  $a'$ , which is neighboring to the SYK site as shown in Fig. 12(b). This state  $a'$  may be a different hyperfine state or an electronically excited state as long as the linewidth of the state is sufficiently small. At  $\tau = 0$ , where  $\tau$  denotes the present time during the protocol, the interaction between the qubit atom and the SYK atom is turned on and it is set to be attractive, i.e.,  $\tilde{U}_i < 0$ . At the same time, we apply a  $\pi$ -pulse with frequency  $\omega = E_{a'} - E_{a,1} - \tilde{U}_1$ , which resonantly couples the  $E_{a,1}$  and  $E_{a'}$  states if there is the qubit atom in the left well, i.e., if the qubit state is  $|1\rangle_C$ . Here  $E_{a'}$  denotes the energy of the lowest band of the atoms in another state. Hence, the application of the  $\pi$ -pulse leads to the operation of  $\hat{c}_1$  for the  $|1\rangle_C$  state and that of the identity matrix for the  $|0\rangle_C$  state, thus creating process (ii).

We next turn off the atomic interaction and perform the unitary time evolution of the system until  $\tau = t$ . This corresponds to process (iii). At  $\tau = t$ , we apply a  $\pi$ -pulse with frequency  $\omega = E_{a'} - E_{a,N}$ , which resonantly couples the  $E_{a,N}$  and  $E_{a'}$  states. This corresponds to the operation of  $\hat{c}_N$ , namely process (iv).

Process (v) requires the sign of the Hamiltonian to be inverted. Although such a manipulation is rather hard in usual systems, it can be made for our SYM model simply by inverting the sign of the detuning for all the PA lasers. We perform the unitary time evolution of the inverted Hamiltonian until  $\tau = 2t$ . At  $\tau = 2t$ , we set the atomic interaction to be repulsive ( $\tilde{U}_i > 0$ ) and apply a  $\pi$ -pulse with frequency  $\omega = E_{a'} - E_{a,1}$ , which leads to the operation of  $\hat{c}_1$  for the  $|0\rangle_C$  state and no operation for  $|1\rangle_C$ . This is nothing but process (vi).

In order to obtain  $\langle \hat{X}_C \rangle$ , we need to measure the population of the bonding state in the qubit double well. Such a measurement can be made by means of the band-mapping techniques used in Ref. [37]. On the other hand, in order to obtain  $\langle \hat{Y}_C \rangle$ , we need to measure the current between the two wells, which is possible using the optical lattice microscope techniques [48–51]. Thus, process (vii) is feasible.

It has been also suggested that the degeneracy of the ground state in the SYK model can be read off from the low-temperature behavior of the single-particle Green's functions [31],

$$G_{i,j}(t) = \langle \hat{c}_j^\dagger(t) \hat{c}_i(0) \rangle. \quad (31)$$

We suggest that  $G_{i,j}(t)$  can be measured in a way very similar to the one described above. Specifically, skipping processes (iv) and (v) corresponds to a protocol to measure  $G_{i,i}(t)$ . The offsite case ( $i \neq j$ ) is also possible simply by replacing  $\hat{c}_i$  operation in process (vi) with  $\hat{c}_j$ .

## V. CONCLUSIONS

We have suggested that ultracold gases in optical lattices can be applied to experimental studies of quantum gravity under the assumption of the holographic principle. As a specific example, we have proposed an experimental design for creating the SYK model, whose low-temperature state has been conjectured to be dual to  $\text{AdS}_2$  black holes [31]. Moreover, we have shown how to measure the OTOC functions and the single-particle Green's function, which characterize black hole properties, with use of a control qubit consisting of an atom in a double well.

We chose our specific example because it looked the simplest one currently available. However, the SYK model is still rather complicated in the sense that it has an unnatural two-body hopping that has to be Gaussian random. Hence, it will be useful to explore its simplified variants or other quantum gauge models with holography that can be created more easily in optical-lattice experiments. For example, the randomness of the coupling in the SYK model, which is technically most complicated part for the experimental realization, might be needed only to make the theory analytically solvable. If one could find a simple system without random coupling, then the experimental realization would become much easier. We finally note that while the Hawking radiation is one of the most important issues regarding quantum black holes, whether the Hawking radiation can be seen in the SYK model is not clear at this stage. Answering to this question will be an imperative task for future theoretical studies. At very least, a variant of the information puzzle, associated to the way that the information is encoded in a black hole [52], should be studied.

## Acknowledgments

The authors thank S. Aoki, G. Gur-Ari, S. Nakajima, M. Sheleier-Smith, S. Shenker, B. Swingle, and Y. Takahashi for discussions. Discussions during the YITP workshop (YITP-W-16-01) on “Quantum Information in String Theory and Many-body Systems” were useful to complete this work. The authors acknowledge KAKENHI grants from JSPS: Grants No. 15H05855 (I.D. and M.T.), No. 25220711 (I.D.), No. 25287046 (M.H.), and No. 26870284 (M.T.).

## Appendix A: Properties of $J_{ij,kl} = (2N)^{3/2} \sum_{s=1}^{n_s} g_{s,ij} g_{s,kl} / \nu_s$

In this appendix we explain basic properties of  $J_{ij,kl} \equiv (2N)^{3/2} \sum_{s=1}^{n_s} \frac{g_{s,ij} g_{s,kl}}{\nu_s}$ . We take  $\nu_s = +\sqrt{n_s} \sigma_s$  for even  $s$  and  $\nu_s = -\sqrt{n_s} \sigma_s$  for odd  $s$ , and the Gaussian weight of  $g_{s,ij}$  is chosen to be  $\frac{e^{-g_{s,ij}^2 / (2\sigma_g^2)}}{\sqrt{2\pi}\sigma_g}$ , with  $\sigma_g^2 / \sigma_s = (2N)^{-3/2} J$ . It will turn out that this corresponds to the Gaussian random coupling  $J_{ij,kl}$  needed for the real-SYK model, with  $J = 1$ . Generic values of  $J$  can be realized by rescaling  $g_{s,ij}$  and/or  $\nu_s$ .

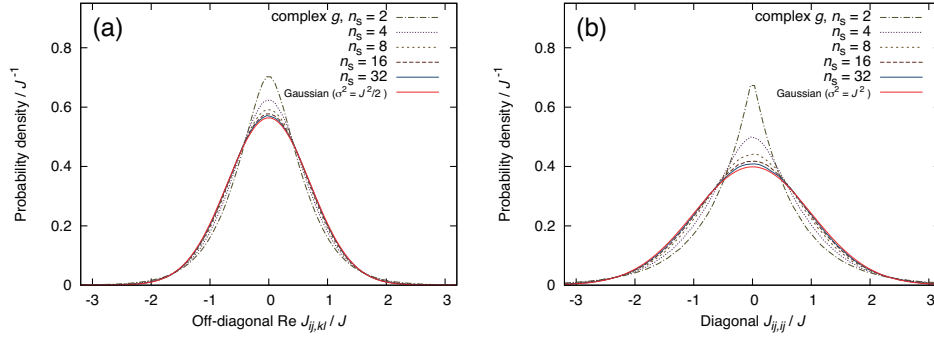


FIG. 14: (a): Distribution of  $J_{ij,kl} = \frac{(2N)^{3/2}}{\sqrt{n_s}J} (\sum_{s:\text{even}} g_{s,ij} g_{s,kl}^* - \sum_{s:\text{odd}} g_{s,ij} g_{s,kl}^*)$  with only the off-diagonal components (i.e.  $(i,j) \neq (k,l), (l,k)$ ); (b): Distribution of the real  $J_{ij,ij} = \frac{(2N)^{3/2}}{\sqrt{n_s}J} (\sum_{s:\text{even}} |g_{s,ij}|^2 - \sum_{s:\text{odd}} |g_{s,ij}|^2)$ . The weights of  $\text{Re}g_{s,ij}$  and  $\text{Im}g_{s,ij}$  are Gaussian with variance  $\sigma_g^2 = (2N)^{-3/2} J^2/2$ ,  $\frac{e^{-|\text{Re}(\text{Im})g_{s,ij}|^2/(\sigma_g^2)}}{\sqrt{\pi}\sigma_g}$ . The distribution of  $\text{Re}J_{ij,kl}$  converges to  $\frac{e^{-(\text{Re}J_{ij,kl})^2/(J^2)}}{\sqrt{\pi}J}$ , which is shown in (a) as “Gaussian ( $\sigma^2 = J^2/2$ )”. The distribution of  $J_{ij,ij}$  converges to the standard normal distribution (for  $J = 1$ ),  $\frac{e^{-J_{ij,ij}^2/(2J^2)}}{\sqrt{2\pi}J}$ , as shown in (b).  $N = 10$ . The numbers of samples taken are  $10^4$  (a) and  $10^5$  (b), respectively.

Firstly let us show that the distribution of  $x \equiv J_{ij,kl}$  converges to  $e^{-x^2}/\sqrt{\pi}$  for  $(i,j) \neq (k,l)$  and  $e^{-x^2/2}/\sqrt{2\pi}$  for  $(i,j) = (k,l)$ . Then, we should show that, when real numbers  $x_s$  and  $y_s$  are distributed with the weight  $\frac{e^{-x_s^2/2}}{\sqrt{2\pi}}$  and  $\frac{e^{-y_s^2/2}}{\sqrt{2\pi}}$ , (1)  $\frac{1}{\sqrt{n_s}} \sum_{s=1}^{n_s} x_s y_s$ , and (2)  $\frac{1}{\sqrt{2n_s}} \sum_{s=1}^{n_s} (x_s^2 - y_s^2)$  converge to Gaussian distribution with width 1 and  $\sqrt{2}$ . The statements (1) and (2) are actually equivalent; indeed, by using  $X_s \equiv \frac{x_s + y_s}{\sqrt{2}}$  and  $Y_s \equiv \frac{x_s - y_s}{\sqrt{2}}$ , we can rewrite the former as  $x_s y_s = (X_s^2 - Y_s^2)/2$  with the same weight,  $e^{-(x_s^2 + y_s^2)/2} = e^{-(X_s^2 + Y_s^2)/2}$ . Hence we consider only the former. Because the sum with respect to  $s$  can be regarded as a random walk, the distribution should be Gaussian. Then, in order to determine the width, we only have to calculate the average of  $\left(\frac{1}{\sqrt{n_s}} \sum_{s=1}^{n_s} x_s y_s\right)^2$ . It can be evaluated as

$$\left\langle \left( \frac{1}{\sqrt{n_s}} \sum_{s=1}^{n_s} x_s y_s \right)^2 \right\rangle = \left\langle \frac{1}{n_s} \sum_{s=1}^{n_s} x_s^2 y_s^2 \right\rangle = \frac{1}{\pi} \int x^2 y^2 e^{-(x^2 + y^2)/2} dx dy = 1, \quad (\text{A1})$$

which means the width is 1.

We can also show  $\overline{J_{ij,kl} J_{pq,rs}} \propto (\delta_{ip} \delta_{jq} - \delta_{iq} \delta_{jp})(\delta_{kr} \delta_{ls} - \delta_{ks} \delta_{lr}) + (ij \leftrightarrow kl)$ . Let us note that we only have to show  $\overline{J_{ij,kl} J_{pq,rs}} \propto \delta_{ip} \delta_{jq} \delta_{kr} \delta_{ls} + (ij \leftrightarrow kl)$  for  $i < j, k < l, p < q$  and  $r < s$ . It is equivalent to show that  $(\sum_s g_I^{(s)} g_J^{(s)} / \nu_s)(\sum_{s'} g_P^{(s')} g_Q^{(s')} / \nu_{s'}) = 0$  unless  $I = P, J = Q$  or  $I = Q, J = P$ , where indices  $I, J, P, Q$  represents  $(i, j), (k, l), (p, q)$  and  $(r, s)$ . With this notation,

$$\overline{(\sum_s g_I^{(s)} g_J^{(s)} / \nu_s)(\sum_{s'} g_P^{(s')} g_Q^{(s')} / \nu_{s'})} = \sum_{s,s'} \overline{g_I^{(s)} g_J^{(s)} g_P^{(s')} g_Q^{(s')} / (\nu_s \nu_{s'})}. \quad (\text{A2})$$

If  $I \neq J$  or  $P \neq Q$ , we can rewrite it as

$$\sum_{s,s'} \overline{g_I^{(s)} g_J^{(s)} g_P^{(s')} g_Q^{(s')} / (\nu_s \nu_{s'})} = \frac{1}{n_s} \sum_s \overline{g_I^{(s)} g_J^{(s)} g_P^{(s)} g_Q^{(s)}}, \quad (\text{A3})$$

where we used the invariance of the Gaussian weight w.r.t. a flip of sign of any of  $g_I^{(s)}, g_J^{(s)}, g_P^{(s')}, g_Q^{(s')}$  and  $\nu_s^2 = n_s$ . Then, again due to the invariance of the weight w.r.t. a flip of sign of any of  $g^{(s)}$ , unless  $I = P, J = Q$  or  $I = Q, J = P$  the average vanishes. When  $I = J \neq P = Q$ ,

$$\overline{(\sum_s g_I^{(s)} g_J^{(s)} / \nu_s)(\sum_{s'} g_P^{(s')} g_Q^{(s')} / \nu_{s'})} = \overline{(\sum_s g_I^{(s)} g_J^{(s)} / \nu_s)} \cdot \overline{(\sum_{s'} g_P^{(s')} g_Q^{(s')} / \nu_{s'})} = 0 \cdot 0 = 0. \quad (\text{A4})$$

It is a bit tricky to show  $\overline{JJJ} = 0$ ; actually it holds when  $n_s$  is infinity. For simplicity, let us suppose  $I \neq J$ ,  $P \neq Q$ ,  $V \neq W$ . Then,

$$\begin{aligned} & \overline{\left(\sum_s g_I^{(s)} g_J^{(s)} / \nu_s\right) \left(\sum_{s'} g_P^{(s')} g_Q^{(s')} / \nu_{s'}\right) \left(\sum_{s''} g_V^{(s'')} g_W^{(s'')} / \nu_{s''}\right)} \\ &= \sum_s \overline{g_I^{(s)} g_J^{(s)} g_P^{(s)} g_Q^{(s)} g_V^{(s)} g_W^{(s)} / \nu_s^3} \\ &= O(1/\sqrt{n_s}) \rightarrow 0 \quad (n_s \rightarrow \infty). \end{aligned} \tag{A5}$$

For the same reason, we have

$$\overline{JJJJ} = \overline{JJ} \cdot \overline{JJ} + O(1/n_s), \tag{A6}$$

and so on.

We further note that, if we can introduce complex  $g_{s,ij}$ , we may identify  $(2N)^{3/2} \sum_s \frac{g_{s,ij} g_{s,kl}^*}{\nu_s}$  with  $J_{ij,kl}$ , with both the distributions of  $J_{ij,kl}$  (see Fig. 14) and other quantities discussed in the main text quickly approaching the distributions for the complex SYK model as  $n_s$  is increased.

- 
- [1] S. W. Hawking, *Black hole explosions*, Nature **248**, 30 (1974).
  - [2] S. W. Hawking, *Particle Creation by Black Holes*, Commun. Math. Phys. **43**, 199 (1975) [Commun. Math. Phys. **46**, 206 (1976)].
  - [3] S. Dimopoulos and G. Landsberg, *Black holes at the Large Hadron Collider*, Phys. Rev. Lett. **87**, 161602 (2001).
  - [4] S. B. Giddings and S. D. Thomas, *High-energy colliders as black hole factories: the end of short distance physics*, Phys. Rev. D **65**, 056010 (2002).
  - [5] X. Calmet, *A review of quantum gravity at the Large Hadron Collider*, Mod. Phys. Lett. A **25**, 1553 (2010).
  - [6] CMS Collaboration, *Search for microscopic black holes in pp collisions at  $\sqrt{s} = 8$  TeV*, JHEP **07**, 178 (2013).
  - [7] CMS Collaboration, *Search for resonances and quantum black holes using dijet mass spectra in proton-proton collisions at  $\sqrt{s} = 8$  TeV*, Phys. Rev. D **91**, 052009 (2015).
  - [8] CMS Collaboration, *Search for lepton flavour violating decays of heavy resonances and quantum black holes to an  $e\mu$  pair in proton-proton collisions at  $\sqrt{s} = 8$  TeV*, arXiv:1604.05239 [hep-ex] (2016).
  - [9] ATLAS Collaboration, *Search for quantum black hole production in high-invariant-mass lepton+jet final states using pp collisions at  $\sqrt{s} = 8$  TeV and the ATLAS detector*, Phys. Rev. Lett. **112**, 091804 (2014).
  - [10] Our proposal is different from the sonic black hole [11, 12], which models the Hawking radiation with the emission of phonons, in the sense that we aim to build a real black hole in actual quantum gravitational system.
  - [11] W. G. Unruh, *Experimental black hole evaporation*, Phys. Rev. Lett. **46**, 1351 (1981).
  - [12] O. Lahav, A. Itah, A. Blumkin, C. Gordon and J. Steinhauer, *Realization of a sonic black hole analogue in a Bose-Einstein condensate*, Phys. Rev. Lett. **105**, 240401 (2010).
  - [13] G. 't Hooft, *Dimensional reduction in quantum gravity*, Salamfest 1993:0284-296.
  - [14] L. Susskind, *The World as a hologram*, J. Math. Phys. **36**, 6377 (1995).
  - [15] J. M. Maldacena, *The large N limit of superconformal field theories and supergravity*, Adv. Theor. Math. Phys. **2**, 231 (1998) [Int. J. Theor. Phys. **38**, 1113 (1999)].
  - [16] T. Banks, W. Fischler, S. H. Shenker and L. Susskind, *M theory as a matrix model: A Conjecture*, Phys. Rev. D **55**, 5112 (1997).
  - [17] B. de Wit, J. Hoppe and H. Nicolai, *On the Quantum Mechanics of Supermembranes*, Nucl. Phys. B **305**, 545 (1988).
  - [18] N. Itzhaki, J. M. Maldacena, J. Sonnenschein and S. Yankielowicz, *Supergravity and the large N limit of theories with sixteen supercharges*, Phys. Rev. D **58**, 046004 (1998).
  - [19] K. N. Anagnostopoulos, M. Hanada, J. Nishimura and S. Takeuchi, *Monte Carlo studies of supersymmetric matrix quantum mechanics with sixteen supercharges at finite temperature*, Phys. Rev. Lett. **100**, 021601 (2008).
  - [20] M. Hanada, Y. Hyakutake, G. Ishiki and J. Nishimura, *Holographic description of quantum black hole on a computer*, Science **344**, 882 (2014).
  - [21] G. 't Hooft, *A Planar Diagram Theory for Strong Interactions*, Nucl. Phys. B **72**, 461 (1974).
  - [22] M. Greiner, O. Mandel, T. Esslinger, T. W. Hänsch, and I. Bloch, *Quantum phase transition from a superfluid to a Mott insulator in a gas of ultracold atoms* Nature **415**, 39 (2002).
  - [23] H. Moritz, T. Stöferle, M. Köhl, and T. Esslinger, *Exciting collective oscillations in a trapped gas* Phys. Rev. Lett. **91**, 250402 (2003).
  - [24] T. Kinoshita, T. Wenger, and D. S. Weiss, *Observation of a one-dimensional Tonks-Girardeau gas*, Science **305**, 1125 (2004).
  - [25] G. Roati, C. D'Errico, L. Fallani, M. Fattori, C. Fort, M. Zaccanti, G. Modugno, M. Modugno, and M. Inguscio, *Anderson localization of a non-interacting Bose-Einstein condensate*, Nature **453**, 895 (2008).



- [26] M. Aidelsburger, M. Atala, M. Lohse, J. T. Barreiro, B. Paredes, and I. Bloch, *Realization of the Hofstadter Hamiltonian with ultracold atoms in optical lattices*, Phys. Rev. Lett. **111**, 185301 (2013).
- [27] H. Miyake, G. A. Siviloglou, C. J. Kennedy, W. C. Burton, and W. Ketterle, *Realizing the Harper Hamiltonian with laser-assisted tunneling in optical lattices*, Phys. Rev. Lett. **111**, 185302 (2013).
- [28] G. Jotzu, M. Messer, R. Desbuquois, M. Lebrat, T. Uehlinger, D. Greif, and T. Esslinger, *Experimental realization of the topological Haldane model with ultracold fermions*, Nature **515**, 237 (2014).
- [29] U. J. Wiese, *Towards Quantum Simulating QCD*, Nucl. Phys. A **931**, 246 (2014).
- [30] E. Zohar, J. I. Cirac and B. Reznik, *Quantum Simulations of Lattice Gauge Theories using Ultracold Atoms in Optical Lattices*, Rept. Prog. Phys. **79**, no. 1, 014401 (2016).
- [31] S. Sachdev, *Bekenstein-Hawking Entropy and Strange Metals*, Phys. Rev. X **5**, no. 4, 041025 (2015).
- [32] Talks by A. Kitaev, <http://online.kitp.ucsb.edu/online/entangled15/kitaev/> and <http://online.kitp.ucsb.edu/online/entangled15/kitaev2/>.  
For further details, see also: J. Maldacena and D. Stanford, *Comments on the Sachdev-Ye-Kitaev model*, arXiv:1604.07818 [hep-th].
- [33] S. Sachdev and J. Ye, *Gapless spin-fluid ground state in a random quantum Heisenberg Magnet*, Phys. Rev. Lett. **70**, 3339 (1993).
- [34] S. Sachdev, *Holographic metals and the fractionalized Fermi liquid*, Phys. Rev. Lett. **105**, 151602 (2010).
- [35] K. M. Jones, E. Tiesinga, P. D. Lett, and P. S. Julienne, *Ultracold photoassociation spectroscopy: Long-range molecules and atomic scattering*, Rev. Mod. Phys. **78**, 483 (2006).
- [36] J. Sebby-Strabley, M. Anderlini, P. S. Jessen, and J. V. Porto, *Lattice of double wells for manipulating pairs of cold atoms*, Phys. Rev. A **73**, 033605 (2006).
- [37] M. Anderlini, P. J. Lee, B. L. Brown, J. Sebby-Strabley, W. D. Phillips, and J. V. Porto, *Controlled exchange interaction between pairs of neutral atoms in an optical lattice*, Nature **448**, 452 (2007).
- [38] J. Maldacena, S. H. Shenker and D. Stanford, *A bound on chaos*, arXiv:1503.01409 [hep-th] (2015).
- [39] This Hamiltonian is the one with complex fermion [31], which is slightly different from the one which uses real fermions [32]. They are equivalent at the large- $N$  limit with fixed  $J$ , after the disorder average is taken.
- [40] It may still be possible that the SYK model is not an exact dual of string theory. Even then, the model would provide us with a consistent ultraviolet completion of classical gravity. Moreover, our proposal would still have an important meaning that it could lead to an experiment of a strongly chaotic quantum system which saturates the bound of the Lyapunov exponent proposed in [38].
- [41] W. Fu and S. Sachdev, *Numerical study of fermion and boson models with infinite-range random interactions*, arXiv:1603.05246v2 [cond-mat.str-el] (2016).
- [42] H. P. Büchler, M. Hermele, S. D. Huber, M. P. A. Fisher and P. Zoller, *Atomic quantum simulator for lattice gauge theories and ring exchange models*, Phys. Rev. Lett. **95**, 040402 (2005).
- [43] T. Köhler, K. Góral, and P. S. Julienne, *Production of cold molecules via magnetically tunable Feshbach resonances*, Rev. Mod. Phys. **78**, 1311 (2006).
- [44] Y. Nakajima, H. Inaba, K. Hosaka, K. Minoshima, A. Onae, M. Yasuda, T. Kohno, S. Kawato, T. Kobayashi, T. Katsuyama, and F.-L. Hong, *A multi-branch, fiber-based frequency comb with millihertz-level relative linewidths using an intra-cavity electro-optic modulator*, Opt. Express **18**, 1667 (2010).
- [45] H. Inaba, K. Hosaka, M. Yasuda, Y. Nakajima, K. Iwakuni, D. Akamatsu, S. Okubo, T. Kohno, A. Onae, and F.-L. Hong, *Spectroscopy of  $^{171}\text{Yb}$  in an optical lattice based on laser linewidth transfer using a narrow linewidth frequency comb*, Opt. Express **21**, 7891 (2014).
- [46] M. Takamoto, I. Ushijima, M. Das, N. Nemitz, T. Ohkubo, K. Yamanaka, N. Ohmae, T. Takano, T. Akatsuka, A. Yamaguchi, and H. Katori, *Frequency ratios of Sr, Yb, and Hg based optical lattice clocks and their applications*, C. R. Phys. **16**, 489 (2015).
- [47] B. Swingle, G. Bentsen, M. Schleier-Smith, and P. Hayden, *Measuring the scrambling of quantum information*, arXiv:1602.06271 [quant-ph] (2016).
- [48] N. Gemelke, X. Zhang, C.-L. Hung, and C. Chin, *In situ observation of incompressible Mott-insulating domains in ultracold atomic gases*, Nature **460**, 995 (2009).
- [49] J. F. Sherson, C. Weitenberg, M. Endres, M. Cheneau, I. Bloch, and S. Kuhr, *Single-atom-resolved fluorescence imaging of an atomic Mott insulator*, Nature **467**, 68 (2010).
- [50] C.-L. Hung, X. Zhang, N. Gemelke, and C. Chin, *Slow mass transport and statistical evolution of an atomic gas across the superfluid-Mott insulator transition*, Phys. Rev. Lett. **104**, 160403 (2010).
- [51] T. Fukuhara, A. Kantian, M. Endres, M. Cheneau, P. Schauß, S. Hild, D. Bellem, U. Schollwöck, T. Giamarchi, C. Gross, I. Bloch, and S. Kuhr, *Quantum dynamics of a mobile spin impurity*, Nat. Phys. **9**, 235 (2013).
- [52] J. M. Maldacena, *Eternal black holes in anti-de Sitter*, JHEP **0304**, 021 (2003).